Kapton Flexible Technology for V-band Applications

ZHENING YANG, ALEXANDRU TAKACS,
SAMUEL CHARLOT, DANIELA DRAGOMIRESCU

LAAS-CNRS, Université de Toulouse, CNRS, INSA, UPS, Toulouse, France

Abstract. This paper addresses the flexible Kapton technology for V-band applications. The proposed technology allows a fabrication accuracy down to 6 μm with insertion losses in the range of 0.5 dB/mm for coplanar waveguide lines at 60 GHz. Based on measurements results, the impact of humidity on the Kapton is quantified in the millimeter wave spectrum and V-band with the help of dedicated passive devices: ring resonator and antennas. An assembling process is also proposed in order to integrate active devices on flexible supporting Kapton board.

1. Introduction

Nowadays, there are increasing demands for flexible and wearable electronics. Also the targeted frequency dedicated for emerging applications increases. The millimeter spectrum and especially V-band are now addressed for short-range and high bit-rate communications. For such high frequencies, Kapton flexible substrate has become a trusted candidate. The Kapton exhibits: good RF and thermal properties, very good flexibility over a wide temperature range and good tolerance for many chemical solvents. This paper focus on the recent advances in the development of Kapton flexible technology for V-band applications. First, the Kapton technology is shortly described. Exhaustive investigations of the Kapton behavior in V-band including the quantified impact of the ambient humidity are presented in Section III and in Section IV, respectively. To the best of the authors' knowledge, the impact of humidity on the RF performances of passive devices fabricated by using Kapton technology was not yet experimentally characterized in V band. An assembling process of electronic chips by heterogeneous integration on flexible Kapton is also proposed in Section V.

2. Microfabrication Technology

All the structures presented in this paper were fabricated on a 127µm thick Kapton in the clean room by using a photolithography process. The technological process was optimized in order to obtain the best trade-off between the technological accuracy (line width or gap down to 6 µm can be obtained with a very good uniformity and reproducibility) that guaranty the millimeter wave performances and manufacturing cost that should be competitive. The Kapton is patterned on a PDMS-Si support for a negative photoresist spin coating. The metallization of electric pattern (Cr/Cu 50 nm/500 nm) is carried out by an electron beam physical vapor deposition (EBPVD) and then a surface finishing (gold immersion deposits) about a few nanometers is performed to prevent Cu from oxidizing. For V band applications the state of the arts of the available technologies are reported in Table I, The Kapton technology proposed in this paper exhibits very good technological accuracy and moderate RF loss, mandatory for V band applications.

Table I. Flexible Technologies for V band. CPW: CoPlanar Waveguide, MS: MicroStrip line

Substrate	Metallization	Technology	Accuracy	RF loss	Ref
PET	Silver	Inkjet	40 µm	0.4 dB/mm, CPW	[1]
Kapton	Silver	Inkjet	13 µm	1.5dB/mm, CPW	[2]
Kapton	Silver	Inkjet	35 µm	0.6 dB/mm, CPW	[3]
PEN	Silver	Inkjet	20 µm	Not reported	[4]
PerMX	Gold	Photolithography	5 µm	0.5 dB/mm, MS	[5]
LCP	Copper	Photolithography	85 µm	0.12 dB/mm, MS	[6]
Kapton	Copper	Photolithography	6 µm	0.5 dB/mm, CPW	

3. V-band Characterization of Kapton Technology

Multiple passive devices were selected as benchmark for this technology: a ring resonator, a microstrip patch antenna and a crossed slot dipole antenna. All above mentioned devices, represented in Fig. 1, Fig. 2 and Fig. 3, are appropriate for humidity tests due to their intrinsic sensitivity to dielectric property variation.

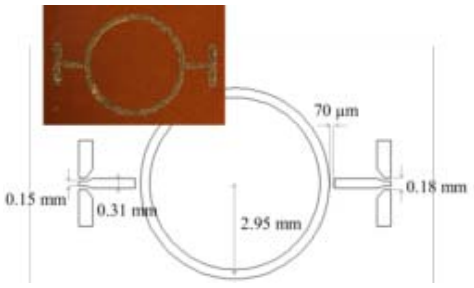

Fig. 1. (Color on line). Ring resonator: mains dimensions and the manufactured device.

The ring resonator is composed by a microstrip ring with the inner radius of 2.95 mm and two microstrip to grounded coplanar waveguide (GCPW) transitions that allows us to perform on-wafer measurements. The same GCPW to microstrip transition was used for the patch antenna. The width of the microstrip ring is 310 µm. There are two 70 µm gaps at the edges of the ring to couple the resonator without overload the test equipment.

The design of a crossed slot dipole antenna is inspired by a printed (coplanar stripline supported) crossed dipole antenna array [7] and the Babinet's principle. CPW feed dimensions of S = 170 µm and G = 12 µm were selected corresponding to the 50 Ohm GSG probe as shown in Fig. 3.

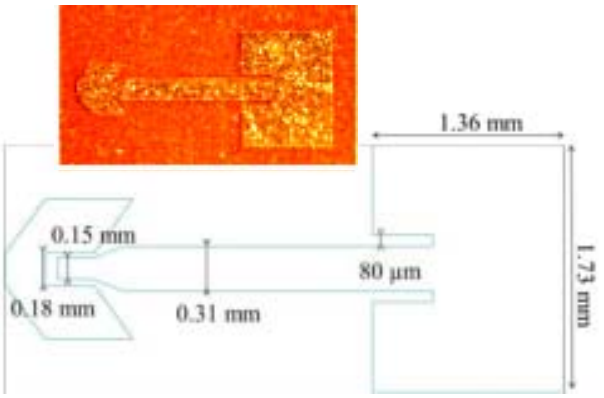

Fig. 2. (Color on line). Microstrip antenna: mains dimensions and the manufactured device.

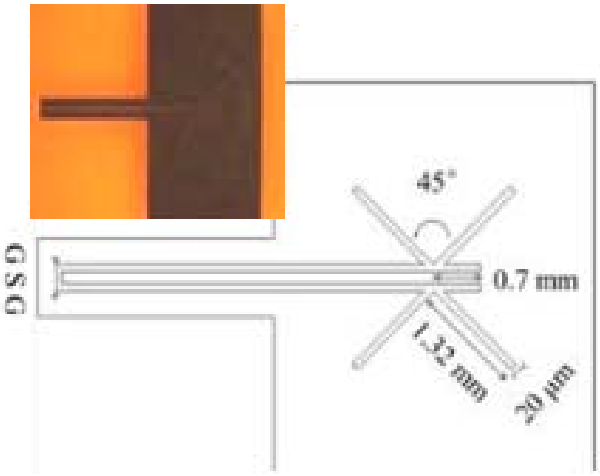

Fig. 3. (Color on line). Crossed slot dipole antenna: mains dimensions and the manufactured device.

4. V-band Humidity Measurement of Kapton

The humidity test method is based on IPC-TM-650 2.6.2.1 standard technique [8]. The test samples were firstly dry out in an oven for over 30 minutes at 150 °C, each of them was individually weighed immediately. Then the test samples were immersed in a crystallizing dish filled with deionized water for 12 hours (h). Each sample was removed independently from the water and sprays dried with nitrogen and weighed again. The same process was repeated for 24 h and 48 h respectively. The weight was increased with 1.64% after 12 h, 1.78% after 24 h and 1.81% after 48 h.

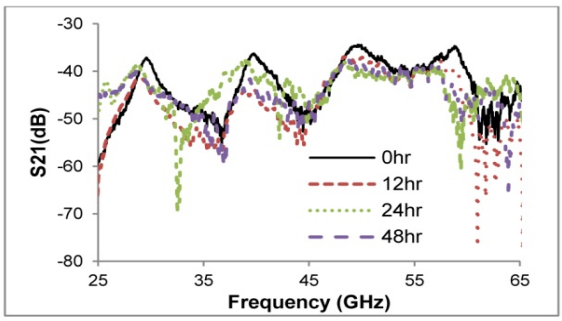

Fig. 4. (Color on line). Measured transmission coefficient of the ring resonator: initial state/0h (continuous black line), measure after 12h (red line, square dot), measure after 24h (green line, circular dot), measure after 48h (violet, dashed line).

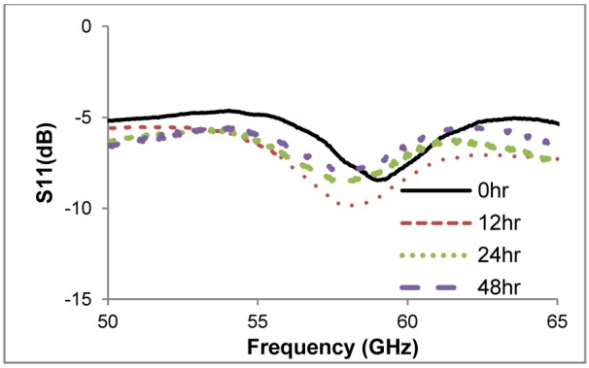

Fig. 5. (Color on line). Measured transmission coefficient of the microstrip patch antenna: initial state/0h (continuous black line), measure after 12h (red line, square dot), measure after 24h (green line, circular dot), measure after 48h (violet, dashed line).

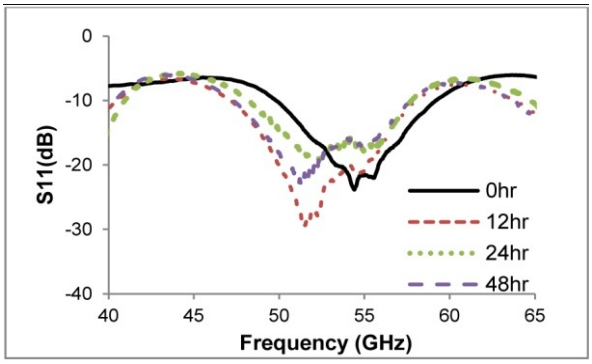

Fig. 6. (Color on line). Measured transmission coefficient of the crossed slot dipole antenna: initial state/0h (continuous black line), measure after 12h (red line, square dot), measure after 24h (green line, circular dot), measure after 48h (violet, dashed line).

The S-parameters measurements were carried out right after the weighing of the samples. Fig. 4 shows the results obtained for the ring resonator, the patch antenna and the crossed slot dipole antenna. The extracted values for the relative dielectric permittivity are reported in Table. II taking into account the associated tolerances.

Table II. Extracted dielectric constant and dielectric loss

Time	ε_r	Tolerance of ε_r	tanδ	Tolerance of tanδ
0 h	3.2	+/– 0.08	0.016	+/– 0.005
12 h	3.4	+/– 0.06	0.03	+/– 0.008
24 h	3.6	+/– 0.08	0.04	+/– 0.006
48 h	3.7	+/– 0.09	0.045	+/– 0.008

Fig. 5 and Fig. 6 show the measured reflection coefficient for the patch and the crossed slot antenna respectively. One can see that the frequency resonance is shifted to the lower frequency because the relative permittivity of the substrate was increased after water immersion as depicted in Table II. Also the S11 decreases because the dielectric losses increase due to water exposition. The input matching of the patch antenna is (only) –8.2 dB mainly due to the transition between microstrip and CPW line. This input matching should appear to be poor but it is not unusual for V-band antennas. For example the coplanar square monopole antenna proposed in [4] presents a measured S11 in the range of –11 dB at 58 GHz despite of the use of an 'intrinsic' CPW excitation. The second antenna (shown in Fig. 6) exhibits better performances: S11 < –20 dB in a 2 GHz bandwidth mainly due to its intrinsic CPW excitation and wideband behavior.

5. Flip Chip Assembling Technique

For the purpose of integration of different components on Kapton polyimide, different dummy circuits were mounted by using a flip chip technique [9] as followed: (i) gold stud ball bumping on chip, (ii) underfilling Kapton structure with an electrically non-conductive paste, (iii) chip with stud bump picked and placed to the Kapton structure by a flip-chip machine, (iv) thermal compression bonding. Four probe method was used to characterize the bumps resistivity as shown in Fig. 7. A resistance about 10 mΩ was measured for the gold bump, which proves a very good DC contact.

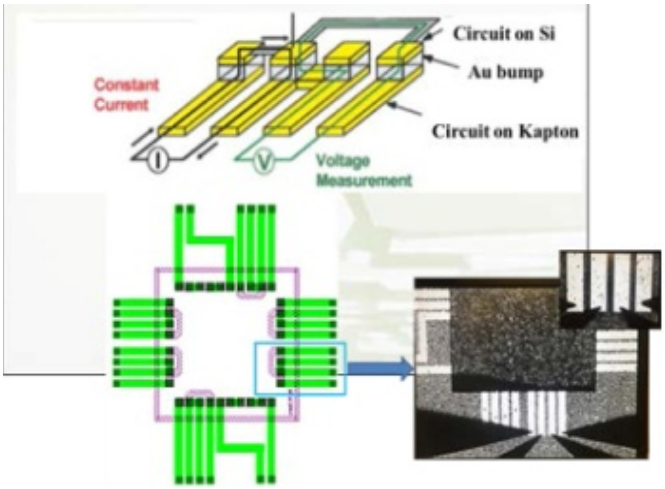

Fig. 7. (Color on line). Four probe method resistivity measurement.

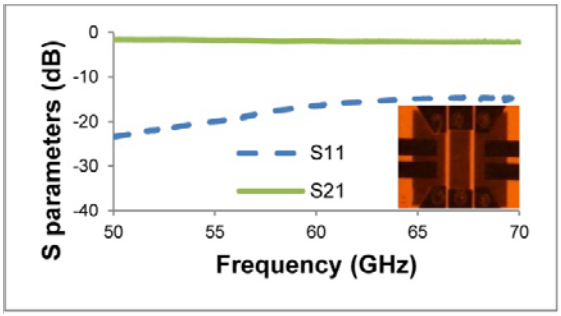

Fig. 8. (Color on line). Measured S-parameters of dummy CPW transmission line mounted on Kapton by using flip chip.

For the RF performance evaluation, firstly a 50 Ω dummy CPW transmission line on was mounted on Kapton as shown in Fig. 8). The measurement results of S-parameters show us a good RF performance. Then a home-designed V-band LNA manufactured by using 65 nm CMOS technology [10] was mounted on Kapton. Its dimension is about 400 µm x 400 µm large and 800 µm height. The pad size (both for RF and DC contacts) are 80µm x 80 µm. This chip is a 'worst case' from an assembling point of view because of its size (foot print of 400µm x 400 µm), aspect ratio (2) and pads size (80µm). The supporting Kapton structure is composed by 50Ω GCPW used as RF In and RF Out and DC pads as shown in Fig. 9.

During our first tests, only the interface between chip and substrate was filled with nonconductive paste (Epotek 353NDT, relative dielectric permittivity of 3.17 and dielectric loss tangent of 0.005 at 1 kHz), which is not robust enough. The chip was fallen apart from the substrate after several bending test. So we added some extra paste around the chip (Permabond UV625, relative dielectric permittivity of 4 at 1 MHz, dielectric loss tangent not known) to ensure the bonding. But this paste changes significantly the characteristic impedance of grounded coplanar line and degrades the RF performances of our LNA. The RF behavior of those pastes (Epotek 353NDT and Permabond UV625) was never investigated in V-band and we suppose that it is too lossy at such high frequencies. Works are under run in order to avoid this drawback by: (i) controlling the nonconductive paste deposition in order to minimize its impact of the CPW line, (ii) using a nonconductive paste with a better RF behavior.

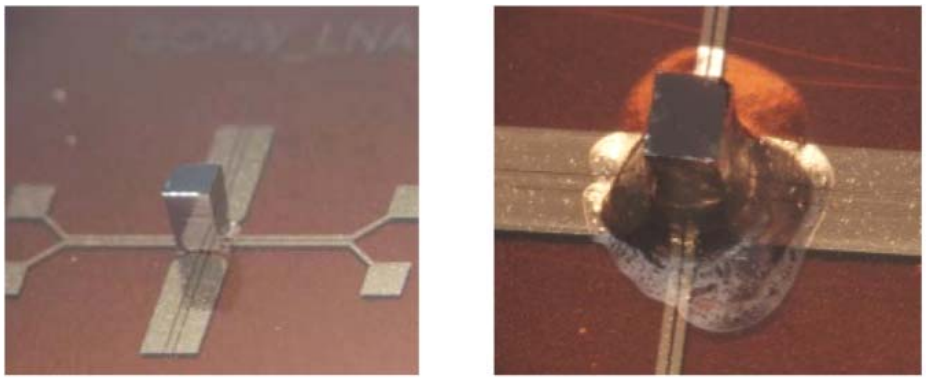

a) b)

Fig. 9. (Color on line). LNA chip mounted on the Kapton supporting structure: (a) by using only Epotek 353NDT under the LNA chip, (b) by adding Permabond UV625 around the LNA chip

6. Conclusion

In this paper, several resonant passive devices were fabricated on Kapton flexible substrate. A standard humidity test was performed in V band. The experimental results demonstrates that the dielectric constant of the Kapton increases with maximum 15.6 % (up to 3.7 from 3.2 the initial value) and the dielectric losses increases with maximum 181% (up to 0.045 from the initial value of 0.016) when the Kapton structure were immersed in water after 48 hours. A limitation of the water absorption was also observed after 24 hours of the water immersion. The DC and RF measurements of dummy circuit mounted with flip chip technique show very promising results for a 3d heterogeneous integration.

References

[1] K. HETTAK, T. ROSS, R. JAMES, A. MOMCIU, and J. WIGHT, *Flexible plastic substrate-based inkjet printed CPW resonators for 60 GHz ISM applications*, 2014 44th European Microwave Conference (EuMC), pp.1194-1197, October 2014.

[2] S. SWAISAENYAKORN, P.R. YOUNG and M. SHKUNOV, *Characterization of ink-jet printed CPW on Kapton substrates at 60 GHz*, Antennas and Propagation Conference (LAPC), pp. 676-678, November 2014.

[3] M.M. BELHAJ, WEI WE, E. PALLECCHI, C. MISMER, I. ROCH-JEUNE and H. HAPPY, *Inkjet printed flexible transmission lines for high frequency applications up to 67 GHz*, 2014 44th European Microwave Conference (EuMC), pp. 1528-1531, October 2014.

[4] A. BISOGNIN, J. THIELLEUX, WEI WEI; D .TITZ, F. FERRERO, P. BRACHAT, G. JACQUEMOD, H. HAPPY, and C. LUXEY, *Inkjet Coplanar Square Monopole on Flexible Substrate for 60-GHz Applications*, Antennas and Wireless Propagation Letters, IEEE, **13**, pp. 435-438, 2014.

[5] S. SEOK and J. KIM, *Design, Fabrication, and Characterization of a Wideband 60 GHz Bandpass Filter Based on a Flexible PerMX Polymer Substrate*, Components, Packaging and Manufacturing Technology, IEEE Transactions, **3**, (8), pp. 1384-1389, August 2013.

[6] D. THOMPSON, O. TANTOT, H. JALLAGEAS, G.E. PONCHAK, M.M. TENTZERIS and J. PAPAPOLYMEROU, *Characterization of liquid crystal polymer (LCP) material and transmission lines on LCP substrates from 30 to 110 GHz*, Microwave Theory and Techniques, IEEE Transactions, **52**, (4), pp. 1343-1352, April 2004.

[7] A. TAKACS, H. AUBERT, S. FREDON and L. DESPOISSE, *Design and Characterization of Effective Antennas for K-band Rectennas*, 2015 9th European Conference Antennas and Propagation (EUCAP), pp. 1-4, 2015.

[8] https://www.ipc.org/TM/2-3_2-3-25-1.pdf.

[9] M.M. JATLAOUI, D. DRAGOMIRESCU, M. ERCOLI, M. KRÄMER, S. CHARLOT, P. PONS, H. AUBERT, and R. PLANA, *Wireless communicating nodes at 60 GHz integrated on flexible substrate for short-distance instrumentation in aeronautics and space*, International Journal of Microwave and Wireless Technologies, **4**, pp. 109-117, 2012.

[10] M. KRAEMER, D. DRAGOMIRESCU and R. PLANA, *A low-power high-gain LNA for the 60 GHz band in a 65 nm CMOS technology*, 2009 Asia Pacific Microwave Conference (APMC), pp. 1156-1159, December 2009.